Article:

Goode, JB, Hambley, DI and Hanson, BC orcid.org/0000-0002-1720-1656 (2019) A benchtop comparison of drying methods relevant to failed spent nuclear fuel. Progress in Nuclear Energy, 115. pp. 120-125. ISSN 0149-1970

https://doi.org/10.1016/j.pnucene.2019.03.025

A Benchtop Comparison of Drying Methods Relevant to Failed Spent Nuclear Fuel

James B. Goode[a,*], David I. Hambley[a], Bruce C. Hanson[b]

[a]*National Nuclear Laboratory, Central Laboratory, Sellafield, Seascale, Cumbria, CA20 1PG*
[b]*School of Chemical and Process Engineering, University of Leeds, Leeds, LS2 9JT*

Abstract

A drying rig has been constructed to allow detailed comparison of both vacuum drying and flowed gas drying of spent nuclear fuels in response to the upcoming closure of the Thorp reprocessing facility at Sellafield, UK. Drying will be needed ahead of disposal possibly ahead of dry interim storage of stainless steel clad Advanced Gas Reactor fuel.

A large number of tests have been carried out using the same small scale simulated fuel pin. The overall results suggest that the drying rate obtained from vacuum drying is significantly higher than when carrying out flowed gas drying. When energy usage is accounted for the drying efficiency is increased still further.

Testing also considered different defects; pinholes and stress corrosion cracks. Despite the theoretical open area of the crack being potentially greater than for a pinhole, the pinholed samples were found to have a considerably higher drying rate.

Keywords: `nuclear fuel, dry storage, stainless steel, AGR, pinholes, cracks`

---

1. Introduction

The usage of interim dry storage for spent nuclear fuel (SNF) has been practiced for over three decades and in this time two methods of drying fuel have been routinely used; vacuum drying (VD) and flowed gas drying (FGD).

Various different vacuum drying methods are reported. At the Hanford site pond stored zircaloy clad uranium metal fuel has been dried by heating a fuel canister to 50°C and evacuating from 13 to 0.7 mBarA over 24-48 hours [1]. This method was developed to allow the use of a vacuum rebound test to confirm dryness [2] and to avoid thermal excursions during drying.

At Idaho National Laboratory a number of experiments were carried out [3, 4] to develop a method of drying aluminium clad uranium metal fuel from materials test reactors covered with dust and corrosion products leading to the eventual implementation of a method using a 50°C vacuum drying step followed by a high temperature (150°C) purge with argon +2% oxygen to remove uranium hydride [1].

At Chalk River Laboratory in Canada a number of experimental drying tests were carried out on aluminium clad, uranium metal fuel that had been stored in dry wells which were thought to have suffered water ingress. The method used was similar to that at Hanford but at slightly higher temperatures (<100°C) and with the addition of higher pressure heating cycles to increase heat transfer and prevent freezing [5].

The most deployed method of flowed gas drying for spent nuclear fuel (SNF) is Holtec's forced helium dehydration (FHD) system for drying LWR fuel (although other methods do exist). Hot he-

---

[*] Corresponding author

Email address: `James.Goode@NNL.CO.UK` (James B. Goode)

lium is pumped through a storage cask before being dried, reheated and returned to the cask. The parameters are not publicly available but temperatures are below 250°C [6] to prevent damaging the fuel cladding. Pressures are elevated and flow rates are in the region of 100's of kg $hr^{-}1$.

A hot flowed gas method was used to dry magnesium alloy clad uranium metal fuel in France however this involved mechanical stripping of the cladding. The bare uranium was then heated in argon first at 100°C to remove water and then at 430°C to pyrolyse any uranium hydride. A final drying step was carried out at 250°C with an increasing oxygen concentration to partially oxidise the uranium metal.

2. Anticipated Drying Process for Failed Pins

While fuel was traditionally vacuum dried, flowed gas drying was developed in part to prevent overheating shorter cooled fuel with greater decay heat. Under vacuum, when convection is greatly reduced, there is the potential for high temperatures to cause hydride re-orientation in Zircaloy clad fuels leading to premature failure during dry storage.

We can assume that in both cases pins start containing liquid water and the first step in drying is to vaporise this water. When vacuum drying this is achieved by lowering the vapour pressure so, much of the energy required to vaporise the water is already within the system and adiabatic cooling takes place as the water vaporises, within the pin and expands when passing through the defect. This could lead to ice formation. To prevent this additional energy can be supplied by heating the drying vessel itself, however due to the low pressure and gas density there will be little convective heat transfer. Heat must instead be transferred by conduction and radiation. In contrast, flowed gas drying relies upon supplying additional heat to the system to vaporise water. This is achieved by forced convection which is, in this case, a more effective manner of heat transfer than conduction and radiation. The rate of convection can be increased further by increasing the pressure and hence the gas density. While this increases the boiling point of water it will also lead to a lower enthalpy of vaporisation thus potentially increasing the rate of vaporisation.

Once vaporised, the water must be removed, first through the defect and then from the vessel itself in a mass transfer step. In both cases (vacuum and flowed gas drying) the water passes through the defect due to a pressure gradient, with a higher pressure formed when the water vaporises inside the pin. When vacuum drying, water vapour is removed from the vessel by a further pressure gradient towards the vacuum pump while when flowed gas drying the water vapour is removed in the gas flow. In both cases once all liquid water is removed from inside the pin the system is considered to be dry.

Both vacuum drying and flowed gas drying have been used successfully to dry SNF however there has been no consistency in terms of scale, the type and condition of the fuel used or the way in which the outcome was measured. As result it is not possible to ascertain which of the two drying methods is most effective. In order to address this a drying rig has been constructed which is able to carry out both flowed gas and vacuum drying in controlled circumstances and collect detailed data of the drying behaviour. This is being done as the UK's stainless steel (SS) clad AGR fuel will require drying ahead of disposal to a geological disposal facility and may be required if dry interim storage is adopted. This fuel is likely to have relatively little decay heat with much of the fuel having been pond stored for several decades based on current plans[7]. The major concern when drying SNF is failed fuel, that is fuel pins that have become flooded over decades under water. Historically a small proportion of AGR fuel has failed due to intergranular stress corrosion cracking during wet storage [8], prior to the introduction of NaOH as a corrosion inhibitor in the late 1980's. As such microcracking is the recognised form of failure in AGR fuel.

The expectation, and thus a hypothesis that could be tested, was that on this scale vacuum drying will be more effective than flowed gas drying, due to the higher pressure gradient formed by the vacuum pump leading to an increased flow of water vapour from the system. While it is acknowledged that the rate of heat transfer will be lower, with a single pin in direct contact with the vessel walls, the difference is likely to be minimal in comparison to the benefit gained from the greatly reduced vapour pressure. Furthermore the reduced pressure in the system and resultant lower fluid density, will lead to a higher rate of mass transfer across the defect. The work presented here is intended to address this hypothesis by carrying out drying tests with identical simulant fuel pins and as near to identical conditions as is possible. This paper presents the results of all tests carried out as part of the experimental programme with detailed data of specific drying methods presented elsewhere [9]. This programme also compares simulated pins with pinhole defects, as may be formed in the event of pitting corrosion, with microcracked pins.

3. Methodology

The rig used consisted of a heated drying vessel (see fig. 1) with a total volume of $\sim$500 cm^3, an inlet line with a dip-tube and an outlet line from the top of the vessel. When vacuum drying the inlet line was isolated while the outlet line ran to a vacuum pump via an iced water cooled condenser (HX) and a molecular sieve. The ultimate vacuum achievable by the system when dry was $\sim$3.5 mBarA although during most tests the recorded pressure was typically higher (>6 mBarA) due to the presence of water vapour. When flowed gas drying the vacuum pump was replaced by a circulation pump which fed the gas back to the vessel via a circulation heater. The vessel contained thermocouples that could record the vessel gas temperature (VT) and be attached to the test piece to record the surface temperature (ST). The rig is described in greater detail in Goode et al[9].

The majority of tests were carried out with a pinholed stainless steel test piece (SSP TP-fig. 2a). This was made from a short length of stainless steel AGR cladding with a stainless steel plug welded into one end, a stainless steel tube welded into the other end and a Swagleok cap fitted to allow water to be sealed inside. A 300 μm hole

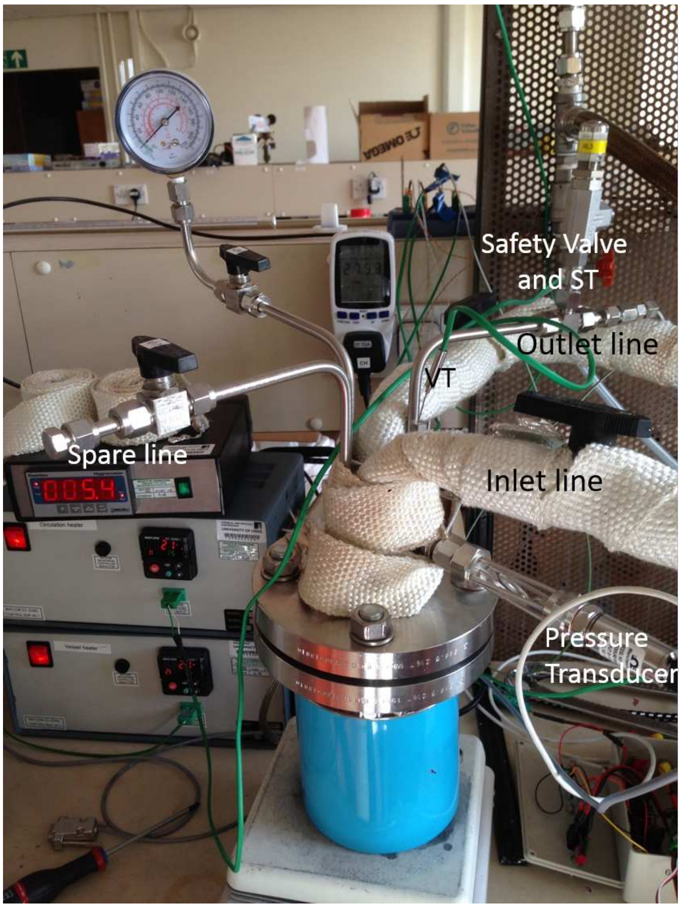

Figure 1: The drying vessel used in the drying tests with various parts labelled.

was drilled into the centre of the section of AGR cladding to represent a pinhole. A second cracked stainless steel test piece (CSS TP-fig. 2b) was used for a smaller number of tests. This consisted of a length of stainless steel tube treated to induce four stress corrosion cracks running axially along the TP (see fig. 2c) with a width of ∼20 μm with such cracks believed to be representative of the failures observed in AGR fuel. The production of this TP is described elsewhere[10] but was essentially carried out by compressing a length of tube radially while boiling in magnesium chloride. The total volume inside each TP is similar being close to 7 cm^3. Since the TP's were not heated internally they simulate fuel with zero decay heat. The temperature of AGR fuel in dry storage would depend on the quantity of fuel in the canister, the burnup and cooling time, however modelling suggested that a typical dry storage cask containing 96 fuel elements with 25 GWd teU^{-}1 (slightly lower than would be expected for future arisings) peak clad temperatures could be up to 108°C after three years cooling, dropping to 68°C after ten years.

Following a number of initial trials, vacuum drying tests were carried out with the vessel wall heater (VH) set to 30°C for the majority of tests although some tests were carried out at 60°C. For the SSP TP the test length was typically 1 hour although a small number of other times were used to investigate the impact of test length. For the CSS TP the test length was between 1 and 6 hours.

For the flowed gas drying testing the set point of the vessel wall heater was typically 125°C although a very small number of tests were carried out at 135°C. The temperature of the circulation heater for the flowed gas was set to the same value. The gas pump was capable of pumping 11 l min^{-1} of air at atmospheric pressure. The flowed gas drying tests typically lasted 6 hours using air. Sequences of 125°C flowed gas drying tests were carried out at pressures ranging 1-2.1 BarA.

The TP was weighed at the beginning and end of each test and the mass of water lost was calculated. A drying rate was then calculated by dividing the mass change by the actual test time thus

(a) SSP TP with pin hole highlighted

(b) CSS TP

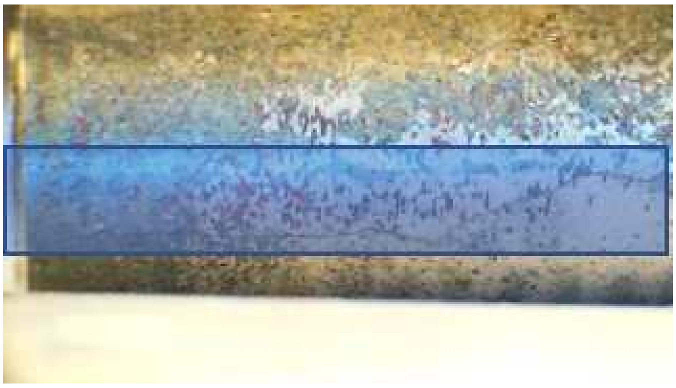

(c) The tube used to produce the CSS TP showing one of the four cracks.

Figure 2: The test pieces used in the drying tests.

allowing a comparison of different drying tests. The tests were typically carried out as part of a sequence that began with the TP full of water for the first test in a sequence. The TP was not refilled with water for the next test until the TP was completely dry.

For the flowed gas drying tests power meters were fitted to the vessel heater, circulation heater and circulation pump. This allowed the energy usage and a drying efficiency to be calculated for each test. Two extended (~6 hours) 30°C vacuum drying drying tests were carried out of similar duration to the flowed gas drying tests with power meters fitted to the vacuum pump and vessel heater.

4. Results

Figure 3 shows the drying rates for the SSP TP when vacuum drying at 30°C and 60°C. The data is plotted in relation to the mass of water that was inside the TP at the beginning of the test. Unsurprisingly the 60°C tests produced higher drying rates than 30°C degree drying tests. The variation in drying rates is substantially greater at 60°C than at 30°C. On the whole the drying rate at 60°C is roughly twice that at 30°C.

At both temperatures the greater the starting mass the higher the drying rate. At 30°C the drying rate remains relatively constant when the TP contains <4 g of water. The drying rate appears to be related to the mass of water within the TP at both temperatures with a high drying rate when the TP is full, levelling out as lower starting masses are reached with this mass varying from around 4 g for 30°C tests to 3 g for the 60°C tests.

The low value observed for 30°C with a starting mass of ~0.2 g is a result of the all water being removed during the test thus giving an artificially low value. This is seen again periodically in further tests.

A number of 30°C tests were carried out at 0.5 and 2 hours using a full TP to investigate the impact of test time (fig. 4). This found that shorter drying tests gave higher drying rates and the variation was considerably greater at shorter times.

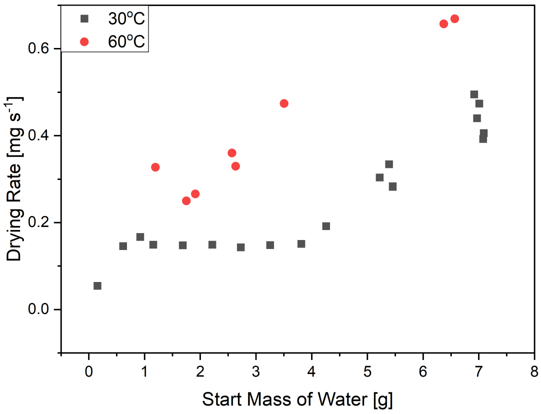

Figure 3: Vacuum drying rates for the SSP TP at 30°C and 60°C.

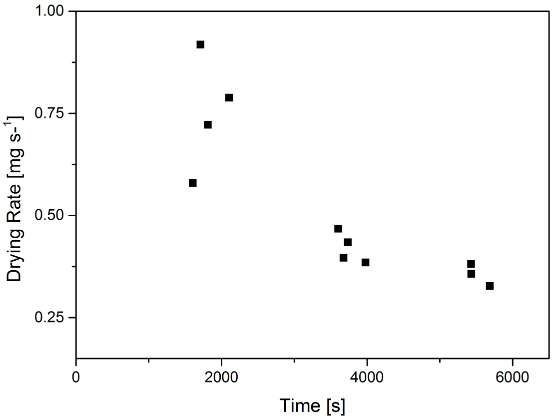

Figure 4: Vacuum drying rates for the SSP TP with a full starting volume (~7 ml) at 30°C and different test times.

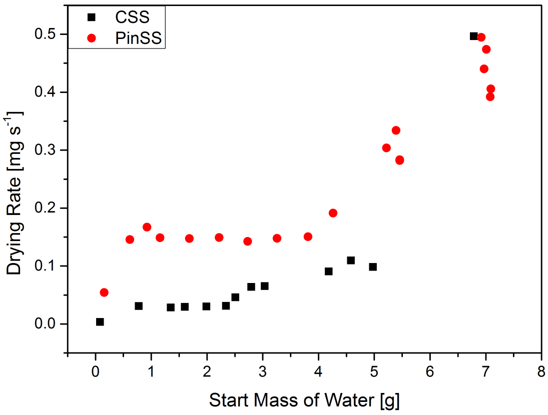

Figure 5: Vacuum drying rates for the CSS and SSP TP at 30°C.

The effect of the defect is seen in fig. 5. The drying rate for the SSP TP is around 0.15 μg s^{-1} while for the CSS TP the drying rate is reduced to 0.1 μg s^{-1} and lower. The step observed at 2.5 g of water for the CSS TP is a result of the test time being extended.

Figure 6 shows the drying rates for the SSP TP at different pressures and temperatures. At the highest pressures (1.9-2.1 BarA) the drying rate is typically higher than at the lower pressures (1-1.5 BarA). Temperature is clearly seen to be the greatest factor as the hottest tests yield the highest drying rate despite higher pressures being used at lower temperatures.

A comparison of the drying rates for the CSS and SSP TP under vacuum drying and flowed gas drying is in fig. 7. It is clear that for both TP's the drying rate when vacuum drying is much higher than when undertaking flowed gas drying.

The drying efficiencies and rates for the two extended vacuum drying tests are shown in fig. 8 alongside the drying efficiencies for the two flowed gas drying tests with the highest drying rate (125°C and 135°C at1.9 BarA). The drying rates for all four tests is roughly similar at ~0.2 μg s^{-1} however the drying efficiency which accounts for energy usage is significantly higher for the vacuum drying tests than the flowed gas drying tests.

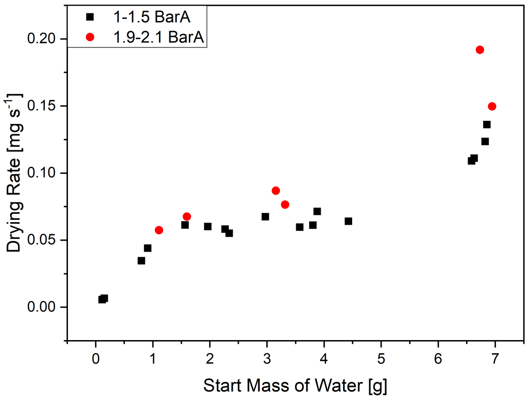

(a) Pressure

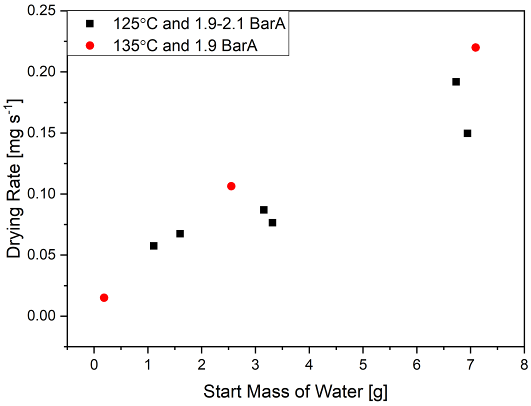

(b) Temperature

Figure 6: Flowed gas drying rates for the SSP TP at different temperatures and pressures.

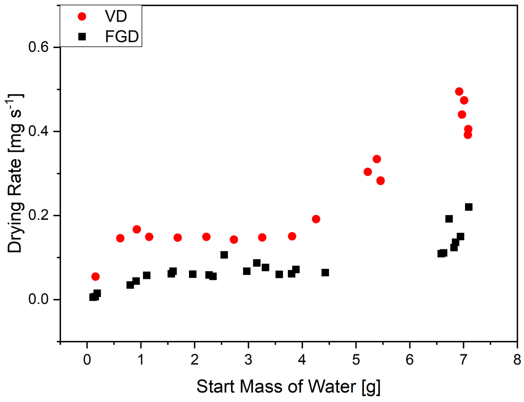

(a) SSP TP

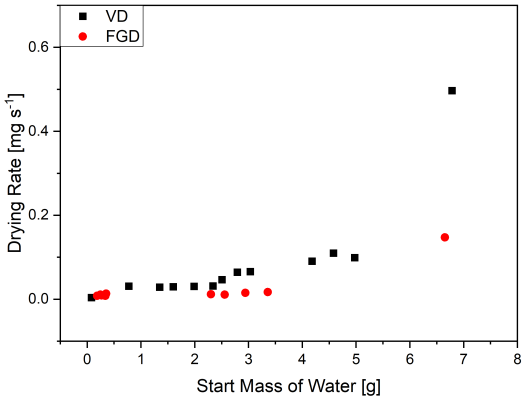

(b) CSS TP

Figure 7: A comparison of vacuum drying and flowed gas drying for the CSS and SSP TP.

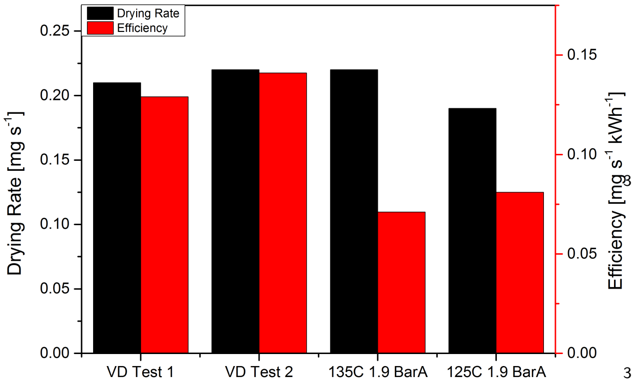

Figure 8: Vacuum and flowed gas drying rates for the CSS and SSP TP at 30°C.

5. Discussion

The vacuum drying tests at different temperatures unsurprisingly show that higher temperatures lead to higher drying rates as heat transfer is improved with a greater temperature gradient. The temperatures used are however low and allow plenty of room for increase.

The reduction in rate as the mass of water within the TP drops is due to liquid water being displaced from inside the TP and then boiling away from the vessel walls. This is a somewhat chaotic process leading to the variation in drying rates between tests. The reduction in rate as the test time is increased when vacuum drying is due to predicted adiabatic cooling of the TP as water is vaporised, reducing the rate of further vaporisation. In this system energy is only replaced by conduction due to contact from the vessel walls to the TP. Real fuel will be self heating and as such there will be less impact from increasing drying time. In flowed gas drying tests the drying rate would be expected to increase with time as the system warms however since the time taken to reach the set point for the circulated gas (as opposed to the vessel walls) was several hours running tests of variable length was not practical.

The initial loss of liquid water from the system is followed by the removal of water by evaporation only and this scenario is more likely when drying real fuel. The drying rates during this phase of drying are typically more consistent.

The impact of pressure on the drying rate when flowed gas drying is likely due to a combination of faster heating and reduced enthalpy of evaporation. At lower pressures the gas density is lower and the gas is therefore less effective as a heat transfer medium leading to the time taken to reach the maximum recorded surface temperature of the TP being reduced in higher pressure tests. The increased pressure also leads to a reduced enthalpy of evaporation. The surface temperature of the TP indicates that only the 1 BarA test led to a surface temperature equal to that of the boiling point with the higher pressure tests being hotter overall but cooler than the boiling point. Since the highest drying rates were for the higher pressures this suggests that a lower enthalpy is more important than ensuring boiling takes place, something that was considered to be a possibility before testing.

The highest rate overall came at the one test sequence carried out at 135°C rather than 125°C but not at the highest pressure. This suggests that temperature is a more important factor.

The drying rate for the CSS TP is significantly lower than that for the SSP TP. Calculations show that the open area of a 20 μm wide crack running along the length of the TP ($\sim$40mm) would theoretically be greater than that of a single 300 μm diameter pinhole and since the production method would lead to up to four cracks forming if the drying rate is based purely on the open area of the defect then it would be reasonable to expect that the two drying rates would at least be similar. For the purposes of this work it is however enough to be aware that the drying rate through the crack is considerably lower yet drying is still achievable.

As discussed above one of the reasons for the the use of flowed gas drying for LWR fuel is that it prevents overheating. For stainless steel clad AGR fuel with an upper operating temperature of 850°C the maximum allowable temperature during drying is significantly higher and unlikely to be reached. This danger is reduced further since current plans do not envisage AGR fuel with significant decay heat being placed into interim dry storage.

The drying efficiencies for the two methods, which accounts for energy usage has shown that for comparable drying rates vacuum drying has a much greater efficiency. Higher temperatures would increase vacuum drying rates considerably and would be unlikely to have a major impact on overall energy usage thus increasing vacuum drying efficiencies further. There is a thought that despite insulation the pipework from the circulation heater to the vessel suffered significant heat loss and the temperature of the gas entering the vessel may not have been as hot as would have been liked. Since the circulation heater was the major contributor to energy use it may be that heating the vessel only and flowing cool gas would lead to similar rates and to an overall efficiency greater than that for vacuum drying but further work would be required to confirm this.

The primary components of a vacuum drying system are a vacuum pump to remove water vapour and a heated vessel although fuel with high decay heat may not require an external heat source. A flowed gas drying system requires a heat source, gas circulation system and gas drying system as well as additional pipework. Since the current recognised method for confirming dryness consists of a vacuum rebound test[11] a flowed gas drying system would also require a vacuum system. This need for additional system means that a flowed gas drying system would likely be more expensive from a capital standpoint. Running costs may also be impacted by the likely need for large quantities of helium even on a recirculating system with gas scavenging capabilities.

6. Conclusions

The purpose of this work was to establish which of the recognised methods of drying spent nuclear fuel is most effective for drying failed fuel with low decay heat. The expectation was that based on the scale vacuum drying would be more effective and the data presented has shown that vacuum drying removes water at a much greater rate than flowed gas drying. Since the temperatures used for the vacuum drying tests were low there is significant room to increase vacuum drying temperatures should that be wished. When energy usage was considered vacuum drying became even more advantageous. The use of real fuel producing its own decay heat, even in only small amounts, would likely increase this advantage further, particularly in the case of AGR fuel where overheating is unlikely. This decay heat would also be in the area required, i.e. inside a flooded pin.

Defect size and morphology has been shown to have a significant impact on drying rate with rough calculations indicating that this is not related to the open area of the defect. Nevertheless it is possible to remove water vapour through defects similar to those expected to be present in failed fuel using both vacuum and flowed gas drying methods.

Acknowledgements

The authors would like to thank the EPSRC for student funding and the National Nuclear Laboratory and the Nuclear Decommissioning Authority for funding the drying rig construction.

[1] W. S. Large, R. L. Sindelar, Review of Drying Methods for Spent Nuclear Fuel, Tech. Rep. WSRC-TR-97-0075, Savannah River Site (US), Aiken, SC 29808 (Oct. 1999).
URL `http://www.osti.gov/scitech/biblio/14490`

[2] A. L. Pajunen, Cold Vacuum Drying Residual Free Water Test Description, Tech. Rep. HNF–1851, Fluor Daniel Hanford Inc., Richland, WA (United States) (Dec. 1997).
URL `http://www.osti.gov/scitech/biblio/10148296`

[3] R. E. Lords, W. E. Windes, J. C. Crepeau, R. W. Sidwell, Drying Studies for Corroded Doe Aluminum Plate Fuels, Tech. Rep. INEL–96/00134; CONF-960804–29, Idaho National Engineering Lab., Idaho Falls, ID (United States) (May 1996).
URL `http://www.osti.gov/scitech/biblio/260992`

[4] J. Crepeau, S. Reese, H. Mcllroy Jr., R. Lords, Drying of Mock Spent Nuclear Fuel Elements, Drying Technology 16 (3-5) (1998) 545–560.

[5] L. Rodrigo, L. Therrien, B. Surette, Low-Temperature, Vacuum-Assisted Drying of Degraded Spent Nuclear Fuel, in: Waste Management, Decommissioning and Environmental Restoration for Canada's Nuclear Activities Current Practices and Future Needs, Canadian Nuclear Society, Ottawa, 2005.

[6] R. Springman, Forced Gas Dehydration (FGD) System for Drying Nuclear Fuel and Waste Packages, 17th Packaging and Transportation of Radioactive Materials Symposium (PATRAM 13), San Francisco (August 2013).

[7] Nuclear Decommissioning Authority, Oxide Fuels - Preferred Option - Publications - GOV.UK, Tech. Rep. SMS/TS/C2-OF/001/Preferred Option (Jun. 2012).
URL `https://www.gov.uk/government/publications/oxide-fuels-preferred-option`

[8] D. Hambley, Technical Basis for Extending Storage of AGR Fuel, in: GLOBAL 2013, Salt Lake City, (September 2013).
URL `https://www.researchgate.net/profile/David_Hambley/publication/279058579_Technical_Basis_for_Extending_Storage_of_the_UK's_Advanced_Gas-Cooled_Reactor_Fuel/links/5589322308aed6bff80b421d.pdf`

[9] J. B. Goode, D. Harbottle, B. C. Hanson, Vacuum drying of Advanced Gas Reactor fuel, Progress in Nuclear Energy 109 (2018) 145–158. `doi:10.1016/j.pnucene.2018.07.011`.
URL `http://www.sciencedirect.com/science/article/pii/S014919701830177X`

[10] James B. Goode, David Harbottle, Bruce C. Hanson, Drying Simulated Advanced Gas Reactor Fuel: Proving the Concept, in: Proceedings of WM 2017, Pheonix, Arizona, 2017.

[11] ASTM, Guide for Drying Behavior of Spent Nuclear Fuel, Tech. Rep. C-1553-16, ASTM International (2016).
URL `http://www.astm.org/Standards/C1553.htm`